

## SYNTHESIS, CHARACTERIZATION AND SORPTION STUDIES OF NITROGEN-DOPED CARBON NANOTUBES

A. O. OSIKOYA<sup>a</sup>, D. WANKASI<sup>a,c</sup>, R. M. K. VALA<sup>a</sup>, C. W. DIKIO<sup>a</sup>, A. O. AFOLABI<sup>b</sup>, N. AYAWEI<sup>c</sup>, E. D. DIKIO<sup>a\*</sup>

<sup>a</sup>*Applied Chemistry and Nanoscience Laboratory, Department of Chemistry, Vaal University of Technology, P. O. Box X021, Vanderbijlpark, South Africa.*

<sup>b</sup>*Department of Civil and Chemical Engineering, College of Science, Engineering and Technology, University of South Africa, Private Bag X6, Johannesburg, South Africa.*

<sup>c</sup>*Department of Chemical Science, Niger Delta University, Wilberforce Island, Bayelsa State, Nigeria*

Nitrogen doped carbon nanotubes were synthesized using cobalt and silver co-catalyst on magnesium oxide support. Their morphological features were studied using Raman spectroscopy, energy dispersive spectroscopy (EDS), scanning electron microscopy (SEM), transmission electron microscopy (TEM), and X-ray diffraction spectroscopy. Equilibrium and thermodynamic batch sorption experiments were carried using concentration, time and temperature effects respectively. The morphological images showed amorphous multiwall nanotubes with crystalline regions that are attributable to the doping of carbon nanotube with nitrogen. The sorption studies indicated a rapid uptake of Cr<sup>3+</sup> by the nitrogen doped carbon nanotubes which was mainly diffusion controlled. The thermodynamic study suggests relatively low temperature (low energy) favoured sorption which is exothermic with a physisorption mechanism.

(Received November 4, 2014; Accepted January 29, 2015)

*Keywords:* Synthesis, Nitrogen, Carbon, Nanotubes, Sorption.

### 1. Introduction

Carbon nanotubes, an allotrope of carbon consisting of hexagonally arranged  $sp^2$  hybridized carbon atoms are currently being widely researched due to its outstanding properties [1,2]. With the emergence of nanoscience and technology in the last decade, research has been initiated to exploit the unusual and unique properties of carbon nanomaterials. Carbon nanomaterials may exist in several forms such as single-walled carbon nanotubes, multi-walled carbon nanotubes, carbon beads, carbon fibres and nanoporous carbon. These different forms of carbon have been studied widely for potential applications in catalyst support, optical devices, quantum computer and biochips. As the name suggests, carbon nanotubes are structurally hollowed cylindrical fibrils of graphitic carbon [2]. This morphological structure makes it (CNT) an excellent research material in the studies of sorbent properties of (especially) new materials. Information on the use of nitrogen doped carbon nanotubes for the removal of metal ions from solution is very scanty which has necessitated this study.

The conventional methods for the removal of metals from aqueous solution and waste water are precipitation, flocculation, filtration, ion exchange reverse osmosis, etc. These methods are very much capital intensive, but some renewable adsorbents have been used for the removal of metals from solutions which include polyvinylchloride, polystyrene, polymethylmethacrylate, seaweeds, medicago sativa (alfafa) and manihot sculenta cranz. [3-8].

---

\* Corresponding author: ezeekield@vut.ac.za

## 2. Experimentation

### Preparation of Catalyst

Cobalt and silver co-catalysts supported on magnesium oxide were used for the synthesis of doped carbon nanomaterial.

500 ml of 1M CoSO<sub>4</sub> solution was reacted with 1000 ml of 1M NaHCO<sub>3</sub> solution at about 55°C to obtain CoCO<sub>3</sub>.

The precipitated CoCO<sub>3</sub> obtained in the reaction above was mixed with 59.5g of MgO while still in the reaction solution, the mixture was then filtered, washed thoroughly with distilled water, and finally dried in the oven at 70°C for about 48 hours and allowed to cool to room temperature.

500ml of 1M AgNO<sub>3</sub> was also reacted with 500 ml of 1M NaCl according to the following equation of reaction:



MgO (71.66 g) was mixed with the reaction product above, the mixture was filtered, washed thoroughly with distilled water and dried in the oven at 120°C for about 12 hours and allowed to cool to room temperature.

### Preparation of carbon nanotubes

Nitrogen doped carbon nanotubes used in this study were synthesized in a horizontal catalytic chemical vapour deposition (CCVD) reactor. The fabrication and experimental setup of this equipment have been described elsewhere [0,7]. These carbon materials were synthesized by pyrolysis of acetylene gas (primary carbon source) and tri-ethyl amine (nitrogen source) via the bubbling method in a tubular quartz reactor which was horizontally positioned within a furnace electronically controlled to produce accurate heating rate and reaction temperature. The prepared catalyst containing the specified loading of both silver and cobalt was loaded in a 120 x 15 mm quartz boat at room temperature and placed in the centre of the quartz reactor which was meticulously placed in the furnace. The furnace (and its contents) was then heated while at the same time purging of the reactor with nitrogen gas flowing at 40 ml/min for about 70 minutes was commenced (to purge the reactor of air and create an inert atmosphere for the synthesis reaction) and allowed to continue until the reaction temperature of 800°C was attained. On the attainment of the synthesis temperature, the nitrogen gas flow was stopped. At the same time acetylene gas flow at 50 ml/min and argon gas flow at 240 ml/min bubbling through tri-ethyl amine were simultaneously introduced into the reactor to start the reaction. The reaction was allowed to proceed for 60 minutes, after when the bubbling of the argon gas through tri-ethyl amine and the acetylene gas flows were stopped. The furnace was allowed to cool to room temperature at the end of reaction period under a continuous flow of nitrogen at 40 ml/min. The samples formed inside the boat were collected.

### Characterization

The structural, morphological and elemental analysis of the synthesized carbon nanotubes were carried out using Raman spectroscopy, FE-SEM, HR-TEM, EDS, and XRD. The Raman spectra were obtained by a Raman spectroscope, Jobin-Yvon HR800 UV-VIS-NIR Raman spectrometer equipped with an Olympus BX 40 attachment. The excitation wavelength was 514.5 nm with an energy setting of 1.2 mV from a coherent Innova model 308 argon-ion laser. The Raman spectra were collected by means of back scattering geometry with an acquisition time of 50 seconds. The surface morphology and EDS measurements were recorded with a JEOL 7500F Field Emission scanning electron microscope. The HR-TEM images of the sample were obtained by a CM 200 electron microscope operated at 100 kV. Powder X-ray diffraction (PXRD) patterns were collected with a Bruker AXS D8 Advanced diffractometer operated at 45 kV and 40 mA with monochromated copper K $\alpha$ 1 radiation of wavelength ( $\lambda = 1.540598$ ) and K $\alpha$ 2 radiation of wavelength ( $\lambda = 1.544426$ ). Scan speed of 1 s/step and a step size of 0.03°. UV-vis spectra were recorded on a Perkin-Elmer lambda 9 UV-vis spectrometer.

### Batch adsorption experiment

**Concentration Effect:** 0.01 g of the carbon nanotube was weighed and placed in pre-cleaned test tubes. Five metal ion solutions with standard concentrations of 20, 40, 60, 80 and 100 mg/l were made from spectroscopic grade standards of  $\text{Cr}^{3+}$  (from  $\text{CrCl}_3$ ). 20 ml of each metal solution were added to each tube containing the carbon nanotube and equilibrated for 1-hour by shaking at 29°C. The carbon nanotube suspensions were centrifuged for 5 min at 4000 rpm. The supernatants were analysed as stated in metal analysis.

**Time Dependent Studies:** 0.01 g of the carbon nanotube was weighed and placed in five pre-cleaned test tubes. Metal ion solution with standard concentration of 60 mg/l was made from spectroscopic grade standard of  $\text{Cr}^{3+}$  (from  $\text{CrCl}_3$ ). 20 ml of the metal solution was added to each tube containing the carbon nanotube and equilibrated for each time intervals of 20, 30, 40, 50 and 60 min respectively by shaking at 29°C. The carbon nanotube suspensions were centrifuged for 5 min at 4000 rpm. The supernatants were analysed as stated in metal analysis.

**Temperature Effect:** 0.01 g of the carbon nanotube was weighed and placed in four pre-cleaned test tubes. Metal ion solution with standard concentration of 60 mg/l was made from spectroscopic grade standard of  $\text{Cr}^{3+}$  (from  $\text{CrCl}_3$ ). 20 ml of the metal solution was added to each tube containing the carbon nanotubes and equilibrated for 1-hour by shaking at temperatures of 25, 40, 60 and 80°C respectively using a Compenstat Gallenhamp water bath. The carbon nanotube suspensions were centrifuged for 5 min at 4000 rpm. The supernatants were analysed as stated in metal analysis.

**Metal Analysis:** The metal analysis was performed by AAS using a Buck Scientific Atomic Absorption/Emission spectrophotometer 200A (AAES). Controls of one of the metal solution were run to detect any possible metal precipitation or contamination.

### Data Analysis

Various equilibrium, kinetic and thermodynamic models (equations) were employed to interpret the data and establish the extent of adsorption. The amount of metal uptake was computed using the material balance equation for batch dynamic studies (equation 1) [3].

$$q_e = \frac{V}{M} (C_o - C_e) \quad (1)$$

with  $q_e$  as metal uptake capacity ( $mg/g$  carbon nanotube at equilibrium),  $C_e$  is metal ion concentration in solution ( $mg/l$ ) at equilibrium,  $C_o$  the initial metal ion solution ( $mg/l$ ),  $V$ , the volume of solution in litres and  $M$ , the dry weight of carbon nanotube used in ( $g$ ).

Langmuir plots were carried out using the linearized equation 2 below

$$\frac{M}{X} = \frac{1}{abC_e} + \frac{1}{b} \quad (2)$$

Where  $X$  is the amount of  $\text{Cr}^{3+}$  adsorbed per mass  $M$  of carbon nanotube in  $mg/g$ ,  $a$  and  $b$  are the Langmuir constants obtained from the slope and intercepts of the plots.

The essential characteristics of the Langmuir isotherm were expressed in terms of a dimensionless separation factor or equilibrium parameter  $S_f$  [8].

$$S_f = \frac{1}{(1+aC_o)} \quad (3)$$

With  $C_o$  as initial concentration of  $\text{Cr}^{3+}$  in solution, the magnitude of the parameter  $S_f$  provides a measure of the type of adsorption isotherm. If  $S_f > 1.0$ , the isotherm is unfavourable;  $S_f = 1.0$  (linear);  $0 < S_f < 1.0$  (favourable) and  $S_f = 0$  (irreversible).

The adsorption intensity of the  $\text{Cr}^{3+}$  in the carbon nanotube was assessed from the Freundlich plots using the linearized equation 4 below

$$\ln \frac{X}{M} = \frac{1}{n} (\ln C_e) + \ln K \quad (4)$$

where  $K$  and  $n$  are Freundlich constants and  $1/n$  is approximately equal to the adsorption capacity.

The fraction of carbon nanotube surface covered by the  $\text{Cr}^{3+}$  was computed using equation 5

$$\theta = 1 - \frac{C_e}{C_o} \quad (5)$$

With  $\theta$  as degree of surface coverage

The effectiveness of the adsorbent (carbon nanotube) was assessed by the number of cycles of equilibrium sorption process required to reduce the levels of  $\text{Cr}^{3+}$  in solution according to the value of the distribution (partition coefficient ( $K_d$ )) in equation 6.

$$K_d = \frac{C_{aq}}{C_{ads}} \quad (6)$$

Where  $C_{aq}$  is concentration of  $\text{Cr}^{3+}$  in solution,  $mg/l$ ;  $C_{ads}$  is concentration of  $\text{Cr}^{3+}$  in carbon nanotube in  $mg/l$ .

The heat of adsorption ( $Q_{ads}$ ) was obtained using the following Suzuki equation.

$$\ln\theta = \frac{\ln K_o C_o}{T^{0.5}} + \frac{Q_{ads}}{RT} \quad (7)$$

with  $T$  as solution temperature (K);  $K_o$  a constant and  $R$  gas constant (8.314 J/K.mol).

The linear form of the modified Arrhenius expression was applied to the experimental data to evaluate the activation energy ( $E_a$ ) and sticking probability  $S^*$  as shown in equation 8.

$$\ln(1 - \theta) = S^* + \frac{E_a}{RT} \quad (8)$$

The apparent Gibbs free energy of sorption  $\Delta G^o$  which is a fundamental criterion for spontaneity, was evaluated using the following equation

$$\Delta G^o = -RT \ln K_o \quad (9)$$

$K_o$  is obtained from the Suzuki equation (Eq. 7).

The experimental data was further subjected to thermodynamic treatment in order to evaluate the apparent enthalpy ( $\Delta H^o$ ) and entropy ( $\Delta S^o$ ) of sorption using equation 10.

$$\ln K_o = \frac{\Delta S^o}{R} - \frac{\Delta H^o}{RT} \quad (10)$$

The expression relating the number of hopping ( $n$ ) and that of the surface coverage ( $\theta$ ) as shown in equation 11 was applied to the experimental data.

$$n = \frac{1}{(1-\theta)\theta} \quad (11)$$

With  $C_o$  and  $C_e$  as initial and equilibrium concentrations in  $mol/cm^3$   $R$ , the gas constant and  $T$ , the solution temperature in K.

### 3. Results and discussion

Generally, Raman spectral showed two major peaks of D and G bands appearing at around 1340 and 1580  $cm^{-1}$ , deriving from in-plane motion of the carbon atoms to provide a signature of carbon nanotubes [11]. The Raman spectral feature of nitrogen doped carbon nanotubes figure 1 has two major peaks at 1326 and 1584  $cm^{-1}$ . Berciaud *et al.* (2009) reported that the Raman spectral signature of carbon nanotubes (1340 and 1580  $cm^{-1}$ ) is very sensitive to strain effects as

well as doping. The appearing of the band at 1526 and 1384  $\text{cm}^{-1}$  in the Raman spectral of our nitrogen doped carbon nanotubes, assigned to the G and D band respectively, shifted because of the doping effect of nitrogen. The obtained Raman spectral feature of nitrogen doped carbon nanotubes could be assigned to the multiwall nanotube because of the absence (weakness) of radial breathing mode (RBM) to be observed, which normally appears between 120 and 250  $\text{cm}^{-1}$  in single wall nanotube. [11-12]. Ferrari (2001) attributed these G and D peaks to  $sp^2$  sites of the carbon based materials.

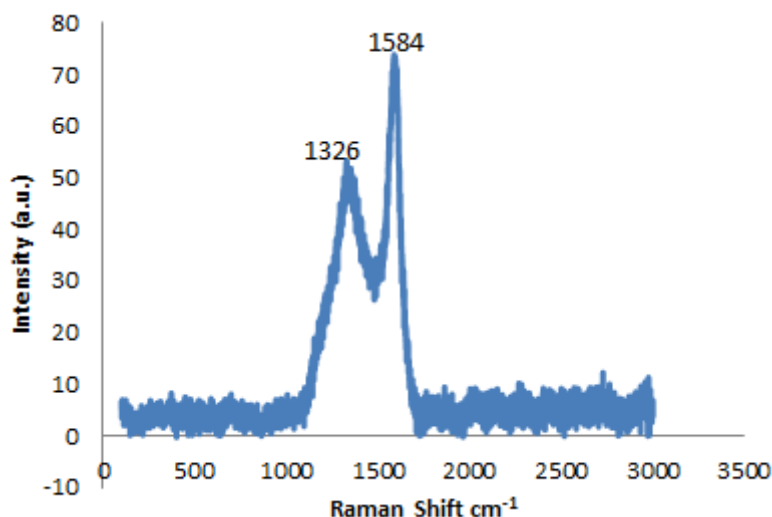


Fig. 1: Raman spectra of as-synthesized nitrogen doped carbon nanotube.

X-ray powder diffraction is a powerful tool for characterizing a solid state sample. Each crystalline substance has a unique X-ray diffraction pattern. With a diffraction pattern an investigator can identify unknown specie or characterize the atomic scale structure of an already identified substance. Figure 2 shows the XRD results of the as-grown carbon nanotubes. The XRD patterns of nitrogen doped carbon nanotubes shows major peaks at around  $2\theta = 25$  and  $44^\circ$ . These peaks are attributed to the hexagonal graphite structures (0 0 2) and (1 0 0), respectively. Therefore, the as-grown carbon nanotubes are amorphous, as also revealed by the SEM and TEM images. Similar results have been reported in the literature by Ci *et al.* (2001) (who called their product amorphous carbon nanotubes) and Li *et al.* (2003). No explanation related to the small and sharp peak around  $2\theta = 33^\circ$  could be found in the literature. However, this peak can be attributed to the crystalline region of nitrogen doped carbon nanotubes.

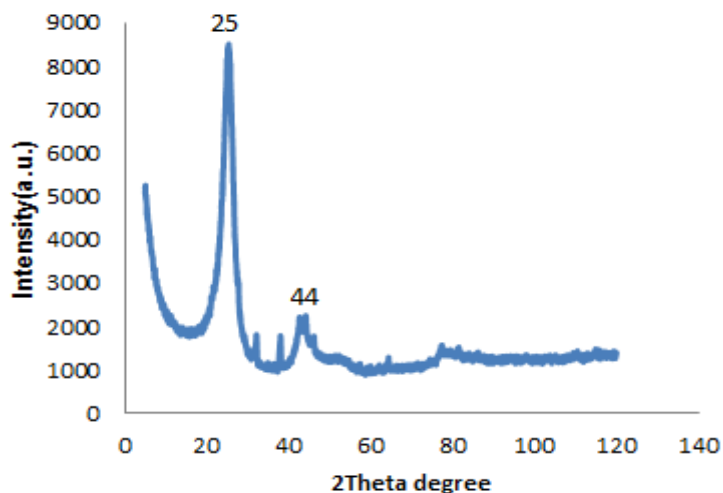


Fig. 2: X-ray diffraction spectrum of the as-synthesized nitrogen doped carbon nanotube

Energy dispersive spectroscopy (EDS) was applied for elemental analysis of the carbon nanotubes. The EDS spectrum presented in figure 3 confirmed sharp peak due to the carbon atom (C), while N and Ag are in trace quantities. The presence of these elements will produce charges on the surface of the nanotubes and create electrostatic forces of attraction between the sample and  $\text{Cr}^{3+}$  in solution.

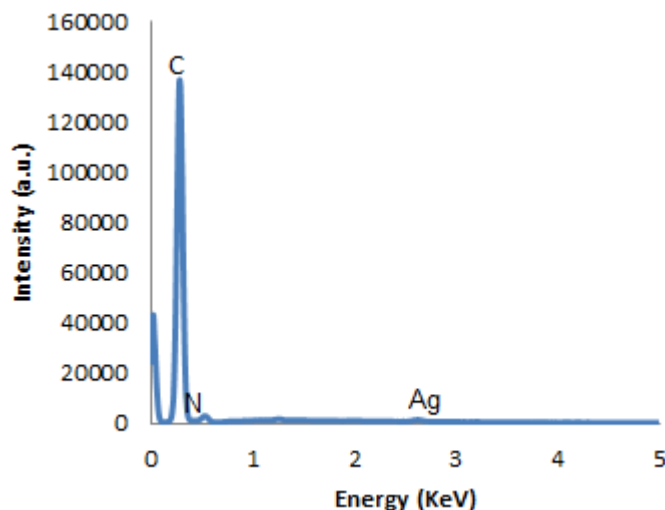


Fig. 3: Energy dispersive spectroscopy (EDS) of the as-synthesized nitrogen doped carbon nanotube

In order to determine the morphology of the carbon nanotubes, scanning electron microscope (SEM), and transmission electron microscope (TEM) images of the sample were taken at a magnification of  $\times 270$ . The SEM and TEM images show that the surface of the carbon nanotubes had irregular small size particles which indicated a high surface area and porous nature as shown in figure 4 and figure 5 (a-d). Large surface area of any adsorbent facilitates maximum adsorption.

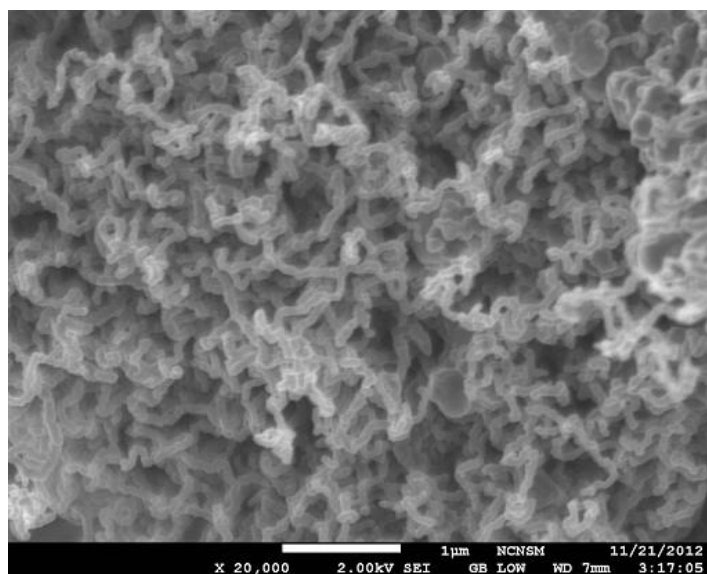


Fig. 4: Scanning electron micrograph of the as-synthesized nitrogen doped carbon nanotube

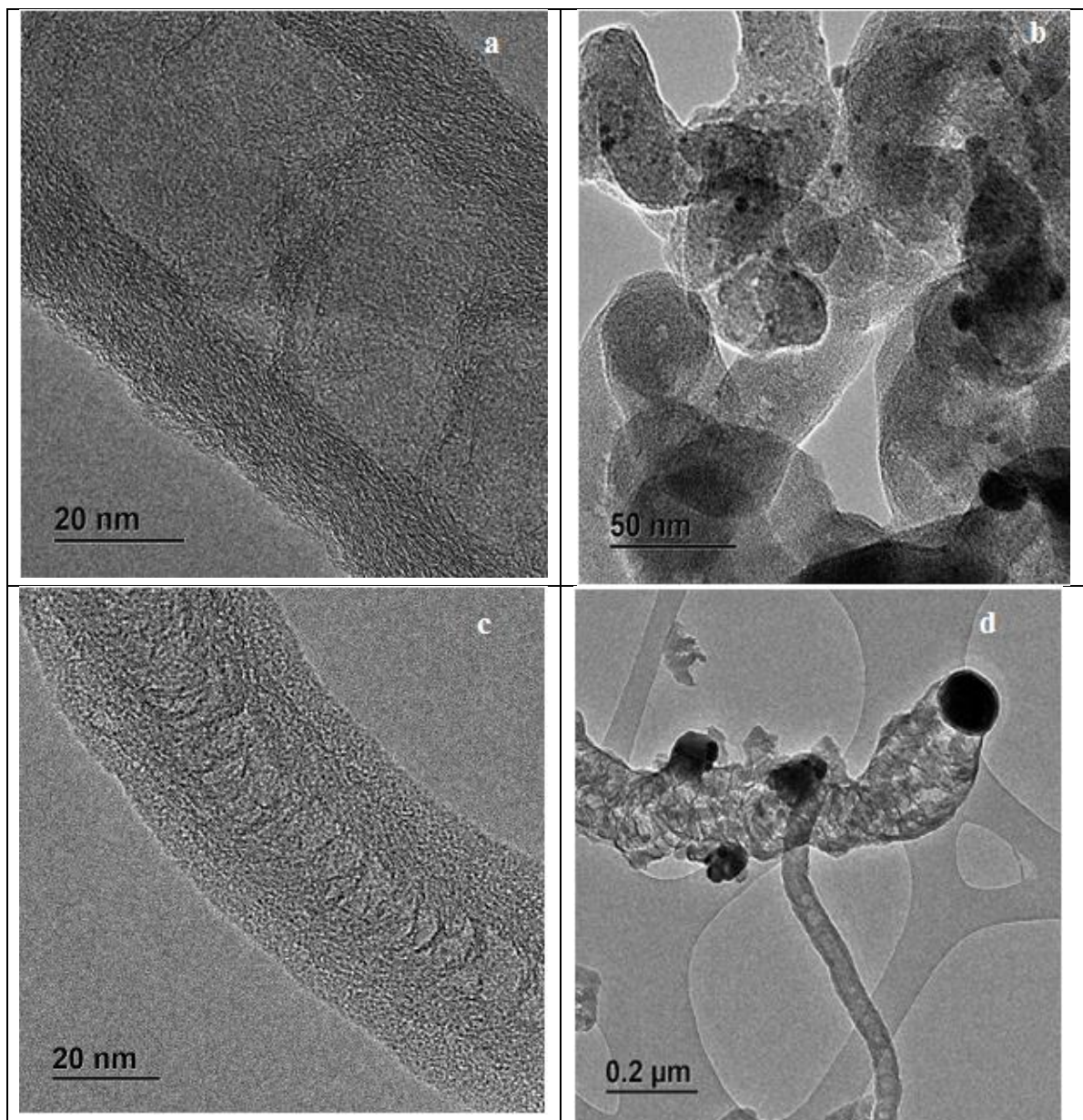


Fig. 5(a-d): Transmission electron micrograph of the as-synthesized nitrogen doped carbon nanotube

The percentage sorption of  $\text{Cr}^{3+}$  by the carbon nanotube at different concentrations of the  $\text{Cr}^{3+}$  is presented in figure 6. The maximum adsorption of 60% took place at equilibrium concentration of  $20 \text{ mg/l } \text{Cr}^{3+}$ . This is because at lower concentration more nanotube pore spaces were available for the  $\text{Cr}^{3+}$ , but as the concentration of  $\text{Cr}^{3+}$  increased, the adsorption capacity of the carbon nanotubes decreased due to reduced availability of free pore spaces. The results indicated that the sorption of  $\text{Cr}^{3+}$  were very much dependent on the concentration of the  $\text{Cr}^{3+}$ .

Time dependency studies show the amount of time needed for maximum adsorption to occur. The variation in percentage removal of  $\text{Cr}^{3+}$  with time has been presented in figure 6. It indicates that a maximum of 48% removal of  $\text{Cr}^{3+}$  was observed in 20 minutes and remained constant afterwards. The relatively short contact time required to attain equilibrium suggests that a rapid uptake of  $\text{Cr}^{3+}$  by the nanotube occurred to fill some of the vacant pores in the carbon nanotube and after which the remaining spaces were difficult to be occupied due to repulsive forces between the Cr ions.

Figure 6 also presents the plot of percentage adsorption of  $\text{Cr}^{3+}$  by the carbon nanotubes at varying temperatures with optimum sorption of 50% occurring at  $28^\circ\text{C}$ . The plot showed that

further increase in temperature resulted in a slight decrease in adsorption. This is in agreement with the general principle that physical adsorption decreases with increase in temperature. [1]. This behaviour could be attributed to the weakening of the attractive forces between the nanotubes and  $\text{Cr}^{3+}$ , the increased kinetic energy of the  $\text{Cr}^{3+}$  and the decrease in the thickness of the boundary layers of the carbon nanotube due to the higher tendency of the  $\text{Cr}^{3+}$  to escape from the pores.

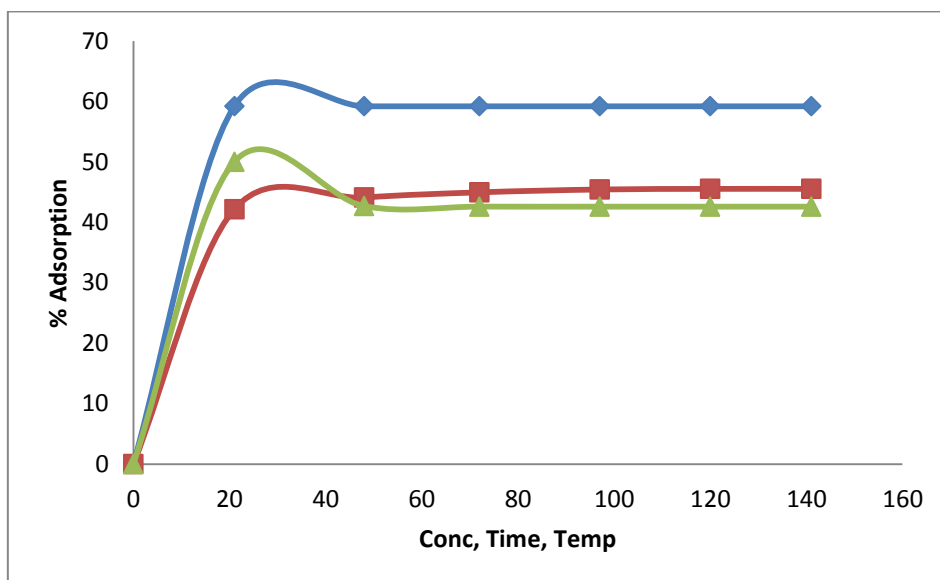


Fig. 6: Adsorption efficiency of  $\text{Cr}^{3+}$  on carbon nanotube with respect to (a)  $\blacklozenge$ -concentration (mg/L), (b)  $\blacksquare$ -Time (min) and (c)  $\blacktriangle$ -Temperature ( $^{\circ}\text{C}$ ).

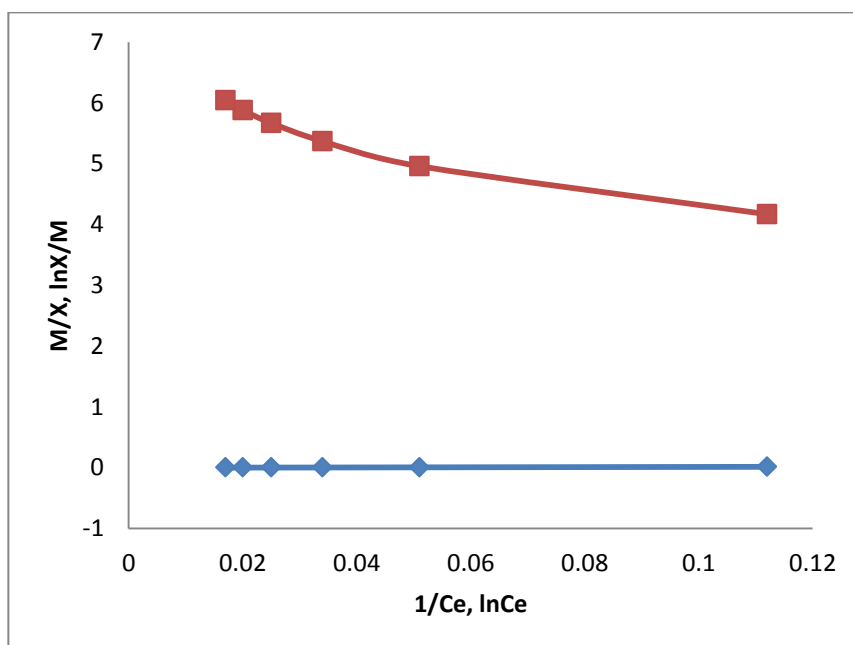


Fig. 7: Equilibrium plots of  $\text{Cr}^{3+}$  adsorbed on nitrogen doped carbon nanotubes (a)  $\blacklozenge$ -Langmuir and (b)  $\blacksquare$ - Freundlich plots.

The extent of adsorption can be correlated by means of an isotherm. Attempts were made to fit the data obtained from the adsorption experiments into various adsorption isotherms. The linear plots of the Langmuir and Freundlich isotherm models for the sorption of  $\text{Cr}^{3+}$  by the carbon nanotubes are presented in figure 7. These straight line plots confirmed the application of the

Langmuir and Freundlich isotherm models to the adsorption of  $\text{Cr}^{3+}$  by the nanotube. The slopes and intercepts were used to compute the Langmuir constants and adsorption capacity.

The fraction of the carbon nanotube surface covered by the  $\text{Cr}^{3+}$  is given as 0.592 (table 1). This value indicates that 59% of the pore spaces of the nanotube surface were covered by the  $\text{Cr}^{3+}$ , which means high degree of adsorption.

Table 1: Equilibrium and thermodynamic parameters

Heat of adsorption $Q_{ads}$ KJ/ molK	Sticking probability $S^*$	Activation energy $E_a$ J/molK	Gibbs free energy of adsorption $\Delta G^o$ KJ/mol	Apparent entropy $\Delta S^o$ J/molK	Apparent enthalpy $\Delta H^o$ J/mol	Surface coverage $\theta$	Separation factor $S_f$	Hopping number $n$	Sorption coefficient $K_d$
-1.39	0.654	-170.0	-0.799	1.870	-171.9	0.592	0.751	4	0.689

In order to determine the nature of the adsorption process, whether favourable or unfavourable, the dimensionless constant separation term  $S_f$  was investigated (equation 3). The result ( $S_f=0.751$ ) in table 1 was less than one and greater than zero which showed that the sorption of  $\text{Cr}^{3+}$  onto the carbon nanotube was favourable.

The effectiveness of the carbon nanotube as an adsorbent for  $\text{Cr}^{3+}$  from solution was assessed through the sorption distribution or partition coefficient  $K_d$  presented in table 1. The value of  $K_d$  (0.687) suggests that the carbon nanotube is an effective adsorbent and that a very few number of cycles of equilibrium sorption process will be required to reduce the levels of  $\text{Cr}^{3+}$  in solution.

In order to calculate the heat of adsorption ( $Q_{ads}$ ) for the sorption of  $\text{Cr}^{3+}$  onto the carbon nanotubes, equation 7 was used. The value of  $Q_{ads}$  ( $-1.39 \text{ KJmol}^{-1}\text{K}^{-1}$ ) is negative as presented in table 1, which indicates that the adsorption was exothermic i.e. low temperatures favour the adsorption of  $\text{Cr}^{3+}$  by the nanotube. Temperature increase did not enhance the sorption process.

The activation energy  $E_a$  and the sticking probability  $S^*$  were calculated from equation 8. The value of  $E_a$  and  $S^*$  were shown in table 1 as  $-170.0 \text{ Jk}^{-1}\text{mol}^{-1}$  and 0.654 respectively. The relatively low and negative  $E_a$  value indicates that low temperature or energy favours the sorption and the adsorption process is exothermic. Relatively low value of  $E_a$  also suggests that the sorption process is diffusion controlled. The sticking probability  $S^*$  indicates the measure of the potential of an adsorbate to remain on the adsorbent. It is often interpreted as  $S^* > 1$  (no sorption),  $S^* = 1$  (mixture of physic-sorption and chemisorption),  $S^* = 0$  (indefinite sticking – chemisorption),  $0 < S^* < 1$  (favourable sticking – physic-sorption). The value of  $S^*$  obtained for the sorption of  $\text{Cr}^{3+}$  by the carbon nanotube was between zero and one which indicates that the adsorption was favourable and followed physic-sorption mechanism.

Table 1 also presents the Gibbs free energy  $\Delta G^o$  for the sorption of  $\text{Cr}^{3+}$  by the carbon nanotubes which was calculated from equation 9. Gibbs free energy is the fundamental criterion of spontaneity. The  $\Delta G^o$  value of  $-0.799 \text{ KJ/mol}$  was negative indicating that the sorption process was spontaneous. The value obtained for  $\Delta G^o$  was also less than  $-20 \text{ KJ/mol}$  suggesting electrostatic interaction between the  $\text{Cr}^{3+}$  and the nanotube which supported physic-sorption mechanism.

The values of the enthalpy change ( $\Delta H^o$ ) and entropy change  $\Delta S$  were calculated from equation 10 to be  $-171.9 \text{ J/mol}$  and  $1.87 \text{ J/molK}$  respectively. A negative  $\Delta H^o$  suggests that sorption proceeded favourably at a lower temperature and the sorption mechanism was

exothermic. A positive  $\Delta S$  suggests that the freedom of the adsorbed  $\text{Cr}^{3+}$  was not restricted in the carbon nanotubes, indicating that physisorption mechanism predominates.

The probability of  $\text{Cr}^{3+}$  finding vacant site on the surface of the carbon nanotube during the sorption was correlated by the number of hopping ( $n$ ) done by the  $\text{Cr}^{3+}$ . The hopping number presented in table 1 is 4. The lower the hopping number, the faster the adsorption.[1]. The low value of  $n$  obtained in this study suggests that the adsorption of  $\text{Cr}^{3+}$  on the nanotube was very fast.

#### 4. Conclusion

Nitrogen doped carbon nanotubes were successfully synthesized and the results of the characterization confirmed amorphous multiwall carbon nanotubes with some crystalline regions due to the doping with nitrogen. The equilibrium and thermodynamic batch adsorption studies recorded rapid uptake of the  $\text{Cr}^{3+}$  by the carbon nanotubes which was diffusion controlled. The adsorption was favoured by low temperature and energy which was exothermic with a physisorption mechanism. The results from this study will add to the knowledge base on the synthesis, characterization and the use of nanotubes for the sorption of metal ions from aqueous solutions.

#### Acknowledgement

This work was supported by a research grant from the Research Directorate of the Vaal University of Technology Vanderbijlpark, South Africa.

#### References

- [1] H. Liu, Y. Zhan, R. Li, X. Sun, S. Desilets, H. Abou-Rachid, L.-S. Lussier Carbon, **48**, 1498 (2010).
- [2] S. Lyu, H. Kim, S. Kim, J.W. Park, C. Lee, Appl. Phys. A, **79**, 697 (2004).
- [3] D. Wankasi, E. D. Dikio, J. Chem. doi.org/10.1155/2014/817527. (2014).
- [4] D. Wankasi, E. D. Dikio, Asian J. Chem. Accepted in-press (2014).
- [5] K. H. Chu, M. A. Hashim, Acta Biotechnol. **21**, (4), 295 (2001).
- [6] J. L. Gardea-Torresdey, J. H. Gonzale, J. L. Tiemann, O. Rodingnuez, G. Gamez, J. Hazard Mater. **57**, 29 (1998).
- [7] M. Horsfall, A. I. Spiff, A. A. Abia, Korean Chem. Soc. **25**, 6. (2004).
- [8] T. Ebbensen, A. Ajayan, H. Huiira, K. Tanigaki, Purification of nanotubes, Nature **367**, 159 (1994).
- [9] A. S. Afolabi, A. S. Abdulkareem, S. D. Mhlanga, S. E. Iyuke, J. Exp. Nanoscience **6**(3), 248 (2011).
- [10] V. J. P. Poots, G. Mckay, J. J. Healy, Removal of basic dyes from effluent using wood as an adsorbent. J. Water Fed., 927, 1978.
- [11] S. Berciaud, S. Ryu, L.E. Brus, T.F. Heinz Nano Lett, **9**(1), 246 (2009).
- [12] A.C. Ferrari, Mat. Res. Soc. Symp. Proc., 675 (2001).
- [13] A. Jorio, M.A. Pimenta, A.G. Souza Filho, R. Saito, G. Dresselhaus, M.S. Dresselhaus New J. Phys., **5**, 139.1 (2003).
- [14] M.S. Dresselhaus, G. Dresselhaus, R. Saito, A. Jorio, Phys. Rep., **409**, 47 (2005).
- [15] L. Ci, B. Wei, C. Xu, J. Liang, D. Wu, S. Xie, W. Zhou, Y. Li, Z. Liu, D. Tang J. Cryst. Growth, **233**, 823 (2001).
- [16] W. Li, C. Liang, W. Zhou, J. Qiu, Z. Zhou, G. Sun, Q. Xin, J. Phys. Chem. B, **107**, 6292 (2003).